Bioactive Materials 2 (2017) 121–130

Contents lists available at ScienceDirect

Bioactive Materials

journal homepage: http://www.keaipublishing.com/en/journals/bioactive-materials/

Smart biomaterials: Surfaces functionalized with proteolytically stable osteoblast-adhesive peptides

Annj Zamuner [a, 1], Paola Brun [b, 1], Michele Scorzeto [c], Giuseppe Sica [a], Ignazio Castagliuolo [b], Monica Dettin [a, *]

[a] Department of Industrial Engineering, University of Padova, Via F. Marzolo 9, 35131, Padova, Italy
[b] Department of Molecular Medicine, University of Padova, Via A. Gabelli 63, 35121, Padova, Italy
[c] Department of Biomedical Sciences, University of Padova, Via U. Bassi 58/B, 35131, Padova, Italy

ARTICLE INFO

Article history:
Received 1 March 2017
Received in revised form
9 May 2017
Accepted 9 May 2017
Available online 18 May 2017

Keywords:
Adhesive sequences
Retro-inverso peptides
Surface grafting
Proteolytic degradation
Osteoblast
TIRF

ABSTRACT

Engineered scaffolds for bone tissue regeneration are designed to promote cell adhesion, growth, proliferation and differentiation. Recently, covalent and selective functionalization of glass and titanium surfaces with an adhesive peptide (HVP) mapped on [351–359] sequence of human Vitronectin allowed to selectively increase osteoblast attachment and adhesion strength in *in vitro* assays, and to promote osseointegration in *in vivo* studies. For the first time to our knowledge, in this study we investigated the resistance of adhesion sequences to proteolytic digestion: HVP was completely cleaved after 5 h. In order to overcome the enzymatic degradation of the native peptide under physiological conditions we synthetized three analogues of HVP sequence. A retro-inverted peptide D-2HVP, composed of D amino acids, was completely stable in serum-containing medium. In addition, glass surfaces functionalized with D-2HVP increased human osteoblast adhesion as compared to the native peptide and maintained deposition of calcium. Interestingly, D-2HVP increased expression of IBSP, VTN and SPP1 genes as compared to HVP functionalized surfaces. Total internal reflection fluorescence microscope analysis showed cells with numerous filopodia spread on D-2HVP-functionalized surfaces. Therefore, the D-2HVP sequence is proposed as new osteoblast adhesive peptide with increased bioactivity and high proteolytic resistance.

1. Introduction

The gain in life expectancy during the twentieth century ranks as one of the most extraordinary social and medical achievements but it is accompanied by an increase in age-related pathologies such as obesity, osteoporosis, bone disorders and allied conditions [1]. As the incidence of bone diseases is increasing steeply, the field of bone tissue engineering is attracting more and more attention. Nowadays, autografts represent the gold standard in bone implant since the histocompatibility and lack of immunogenic reactions guarantee osteogenesis, osteoconduction and osseointegration [2,3]. However, additional surgical procedures and risk of inflammation, infection and chronic pain at donor site complicate autogenous bone implants whereas the limited supply of autografts do not meet the needs for large bone fractures [4,5]. Therefore, engineered substitutes ensuring the biocompatibility, osteoconduction and early implant loading are required [6,7].

Since osseointegration and long-term success of the implant are determined by the complex reactions taking place at the tissue-material interface, in bone tissue engineering one of the most relevant issue is to recreate the ability of autogenous grafts to communicate with the surrounding biological environment. Thus, cell adhesion, proliferation, migration and differentiation are induced by coordinate transmembrane signaling occurring in cells approaching the surface of the implant and are mandatory for implant colonization [8–10]. The growing knowledge about molecular processes driving cell adhesion and growth have focused the treatment of implant surfaces on improving the surface-to-cells interactions, complying with the new approach of “biochemical functionalization”. Different techniques have lately been adopted to optimize biological properties of bone implants [11,12]. One of the most promising approach involves the decoration of surfaces of the

* Corresponding author.
E-mail address: monica.dettin@unipd.it (M. Dettin).
Peer review under responsibility of KeAi Communications Co., Ltd.
[1] These two authors contributed equally to this work.

http://dx.doi.org/10.1016/j.bioactmat.2017.05.004

implant with adhesive sequences or osteogenic growth factors [13] using sophisticated strategies to ensure selective bonds and appropriate and functional spatial orientation [14–19]. The peptides are covalently anchored to different surfaces (i.e. glass, quartz, metal oxides and synthetic polymers) through different techniques depending on the type of chemical groups available on the implant's surface [20,21]. Moreover, additional molecules acting as spacers are used during the anchoring process to immobilize the bioactive peptide while preserving the ideal flexibility for receptor interaction.

Several strategies have been developed for bioactive peptides' grafting: a) the use of aminoalkyltrialkoxysilane to bind the amino groups to oxides; b) the insertion of a thiol group in the biomolecule to exploit the link between this group and gold surfaces; c) the use of titanium substrates coated with polypyrrole; d) the synthesis of copolymers containing poly (L-lysine) as coating for surface linking, or poly (ethylene glycol) conjugated to bioactive peptide [22].

The scientific community however hardly questioned the practicability of bioactive surfaces mainly because adhesive sequences grafted onto biomaterials surfaces might be masked by serum proteins *in vivo* thus nullifying the functionalization.

To overcome this criticism, Battista et al. have recently demonstrated that cells dig into the physisorbed protein layer and gain the submerged chemically bound adhesion motifs to establish a firmer adhesive structure and build thicker stress fibres enhancing the mechanical stability of the cytoskeleton [23]. Actually, the stability of the peptides anchored on functionalized biomaterials toward proteolytic degradation by serum enzymes has not been thoroughly investigated even if one of the main limitations in the use of peptides, either as ligands for cell adhesion or as therapeutics, is the short life-time under physiological conditions [24].

The sensitivity of peptides to enzymatic degradation or hydrolysis have prompted the research in tissue engineering to introduce modified amino acids or amino acids with different configuration in the peptide sequence still maintaining the bioactivity. For example, in the work of Zubrzak P. et al. the substitution of residues Phe, Pro and Trp with β-amino acids in a neuro-peptide ensured resistance still maintaining the bioactivity of the native sequence [25]. Other strategies to increase the stability of peptides concern the use of isosteric amino acids, the introduction of “constraint” (cyclization), the conjugation to carrier molecules and alteration of the peptide bond. Finally, another method for stabilization consists in the substitution of L-amino acids with the corresponding D enantiomers. The synthesis of a retro-inverso (or inverted) peptide, D-amino acids assembled in the reverse order as compared to the parent L-sequence, leads to an analogue in which the side chains are usually arranged similarly to the native peptide [26–30]. Unfortunately, retro-inverted sequences not always maintain the bioactivity of the native peptide [31,32]. In most cases, it was shown that retro-inverso peptides do not induce cytotoxicity when compared to L-enantiomers, nevertheless, cytotoxicity has to be ascertained case by case [33,34].

Among several adhesive peptides individuated for functionalization purposes, RGD (arginine-glycine-aspartic acid) motif, interacting with cell membrane integrins, is one of the most extensively studied. In addition, we have demonstrated that a nonapeptide (HVP) from the h-Vitronectin protein (sequence 352–360) selectively enhances osteoblast adhesion through an osteoblast-specific mechanism which involves interactions with membrane glycosaminoglycans (GAGs) and the heparin binding sites on extracellular matrix (ECM) [9]. In the present study, HVP has been covalently and selectively anchored on glass surfaces with a protocol easily transferable to surfaces widely used in bone tissue engineering such as titanium, titanium alloys, and bio-glasses. In addition, a dimeric analogue (2HVP) was designed in order to increase ionic interactions with cellular GAGs and two HVP retro-inverted sequences (DHVP, retro-inverso peptide of HVP, and D-2HVP, retro-inverso peptide of 2HVP) were synthesized to increase the stability toward proteolytic degradation under physiological conditions. The biological characterization (adhesion, calcium, qPCR assays, and morphological evaluation) of glass surfaces functionalized with L and D peptides is reported and discussed.

2. Materials and methods

2.1. Materials

The solid support Sieber Amide resin and all Fluorenylmethyloxycarbonyl (Fmoc) protected amino acids were from Novabiochem (Merk KGaA, Darmstadt, Germany). The coupling reagents 2-(1H-Benzotriazole-1-yl)-1,1,3,3-tetramethyluronium hexafluorophosphate (HBTU) and1-Hydroxybenzotriazole (HOBt) were from Advanced Biotech (Seveso, Italy). N, N-diisopropylethylamine (DIEA) and piperidine were from Biosolve (Leenderweg, Valkenswaard, The Netherlands). Triethoxysilane (TES), 1,2-ethandithiol (EDT) and acetone were from Sigma-Aldrich (Steinheim, Germany). Solvents for synthesis such as N, N-dimethylformamide (DMF), trifluoroacetic acid (TFA), N-methyl-2-pyrrolidone (NMP) and dichloromethane (DCM) were from Biosolve. Solvents for chromatography such as acetonitrile and TFA (HPLC grade) were from Sigma-Aldrich. Ethanol and methanol were from Avantor Performance Materials (Center Valley, PA, U.S.A.). (3-Aminopropyl) triethoxysilane (APTES 2%) was from Sigma-Aldrich.

2.2. Peptide synthesis

All peptides reported in Table 1 were synthetized with Fmoc chemistry by a Syro I synthesizer (MultiSynTech, Witten, Germany).

The peptide HVP was synthesized and purified as reported in Ref. [35]. The retro-inverted analogues DHVP and D-2HVP were synthesized using D-amino acids. The synthesis of 2HVP, DHVP, D-2HVP and a non-adhesive peptide (name: NAp; sequence: GRADSPGRADSPGRADSPGRADSPK) were carried out on 0.72 mmol/g Sieber Amide resin. The side chain protecting groups were: Arg, Pbf or Pmc; Asn and His, Trt; Asp and Glu, OtBu; Lys, Boc; Ser and Tyr, tBu. The Fmoc removal was accomplished by two treatments with 40% and 20% piperidine/DMF for 3 min and 12 min, respectively. The coupling reaction was carried out using 5 eq. of Fmoc protected amino acid and HOBt/HBTU/DIPEA (5 eq. HOBt/HBTU and 10 eq. DIPEA; 45 min) in DMF. In each synthesis, the loading step was a double coupling, and all the remaining steps were single couplings, in the case of DHVP, and double for 2HVP. The synthesis of D-2HVP was carried out with 8 single couplings, followed by double couplings. The first eighteen coupling of NAp's synthesis were single and all the remaining couplings were double. At the end of chain elongation, after Fmoc deprotection the resin

Table 1
Sequences of synthetic peptides. The underlined sequences refer to D-amino acids. All peptides were synthesized as C-terminal amides.

Name	Sequence
HVP	FRHRNRKGY
2HVP	FRHRNRKGYFRHRNRKGY
DHVP	YGKRNRHRF
D-2HVP	YGKRNRHRFYGKRNRHRF

was washed with DCM and dried for 1 h under vacuum. In order to maintain the side-chain protection, the cleavage of the peptides from the resin was carried out using 15 min treatment in 1% TFA/DCM. The resin was filtered, the reaction mixture concentrated and the crude side-chain protected peptide precipitated with cold water. Side-chain protected peptides were isolated by filtration, dried under vacuum and used for specific and covalent surface functionalization. Otherwise, a part of each peptide was cleaved from the solid support with the contemporary side-chain deprotection using the following mixture: 2.5% H_2O MilliQ, 2.5% TES, and 95% TFA (90 min, under magnetic stirring). After cleavage, the resin was filtered, the reaction mixture concentrated and the crude peptide precipitated with cold ethyl ether. Deprotected peptides were purified by reverse-phase liquid chromatography (HPLC) to high purity grade and characterized by electrospray ionization/time of flight mass spectrometry (ESI-TOF). Purified peptides were used to perform enzymatic degradation's studies.

2.3. Peptide characterization

2.3.1. HVP

The native nona-peptide HVP was characterized as reported in Refs. [35,36].

2.3.2. 2HVP

Twenty-five mg of crude peptide dissolved in 25 mL of MilliQ water were loaded on Jupiter C18 (5 μm, 300 Å, 10 × 250 mm, Phenomenex) and separated in the following conditions: eluent A, 0.05% TFA in MilliQ water; eluent B, 0.05% TFA in CH_3CN; gradient, from 0%B to 10%B in 2 min, and from 10%B to 40%B in 40 min; flow rate, 4 mL/min; detection at 214 nm. The chromatogram of purified peptide was carried out in the following conditions: column, Jupiter C18 (5 μm, 300 Å, 4.6 × 250 mm, Phenomenex); injection volume, 10 μL of 1 mg/mL peptide solution; flow rate, 1 mL/min; eluent A, 0.05% TFA in water; eluent B, 0.05% TFA in CH_3CN; gradient, from 10%B to 30%B in 20 min, detection at 214 nm. The retention time results 11.6 min and the purity grade, 99%. Experimental mass: 2447.43 Da, Theoretical mass: 2447.79 Da (ESI-TOF, Mariner System 5220, Applied Biosystem, Perkin-Elmer, California, USA).

2.3.3. DHVP

Thirty mg of crude peptide dissolved in 15 mL of MilliQ water were loaded on Jupiter C18 (5 μm, 300 Å, 10 × 250 mm, Phenomenex) and separated in the following conditions: eluent A, 0.05% TFA in MilliQ water; eluent B, 0.05% TFA in CH_3CN; gradient, from 0%B to 5%B in 2 min, and from 5%B to 20%B in 45 min; flow rate, 4 mL/min; detection at 214 nm. The chromatogram of purified peptide was carried out in the following conditions: column, Jupiter C18 (5 μm, 300 Å, 4.6 × 250 mm, Phenomenex); injection volume, 10 μL of 1 mg/mL peptide solution; flow rate, 1 mL/min; eluent A, 0.05% TFA in water; eluent B, 0.05% TFA in CH_3CN; gradient, from 10%B to 20%B in 20 min, detection at 214 nm. The retention time results 10.8 min and the purity grade, 99%. Experimental mass: 1232.75 Da, Theoretical mass: 1232.39 Da (ESI-TOF, Mariner System 5220, Applied Biosystem, Perkin-Elmer, California, USA).

2.3.4. D-2HVP

The crude peptide (0.02 mmol) dissolved in 25 mL of MilliQ water were loaded on Vydac C18 (5 μm, 300 Å, 10 × 250 mm, Grace) and separated in the following conditions: eluent A, 0.05% TFA in MilliQ water; eluent B, 0.05% TFA in CH_3CN; gradient, from 0%B to 5%B in 2 min, and from 5%B to 15%B in 40 min; flow rate, 4 mL/min; detection at 214 nm. The chromatogram of purified peptide was carried out in the following conditions: column, Vydac C18 monomeric (5 μm, 300 Å, 4.6 × 250 mm, Grace); injection volume, 20 μL of 1 mg/mL peptide solution; flow rate, 1 mL/min; eluent A, 0.05% TFA in water; eluent B, 0.05% TFA in CH_3CN; gradient, from 8% B to 18%B in 20 min, detection at 214 nm. The retention time results 12.4 min and the purity grade, 97.9%. Experimental mass: 2448.32 Da, Theoretical mass: 2447.82 Da (ESI-TOF, Mariner System 5220, Applied Biosystem, Perkin-Elmer, California, USA).

2.3.5. NAp

The chromatogram of crude peptide was obtained in the following conditions: column, Vydac C18 (5 μm, 300 Å, 4.6 × 250 mm, Grace); injection volume, 30 μL of 1 mg/mL peptide solution; flow rate, 1 mL/min; eluent A, 0.05% TFA in water; eluent B, 0.05% TFA in CH_3CN; gradient, from 0%B to 30%B in 30 min, detection at 214 nm. The retention time results 20.8 min. Experimental mass: 2479.20 Da, Theoretical mass: 2479.59 Da (ESI-TOF, Mariner System 5220, Applied Biosystem, Perkin-Elmer, California, USA). Non-adhesive peptide NAp was used as reference in biological assays.

2.4. Enzymatic degradation

A 1% w/v aqueous solutions of HVP, 2HVP, DHVP and D-2HVP were prepared, and 10% not heat-inactivated fetal bovine serum (FBS; Gibco, Thermo Fisher Scientific) in PBS solution was added to each peptide solution in the ratio 1: 9 (peptide solution: 10% FBS). A reference sample containing only 10% FBS was prepared, too. All samples were kept at 37 °C for 5 h. At the end of the reaction time, each solution was analysed through HPLC in the following conditions: column, Jupiter C_{18} "proteo" (4 μm, 90 Å, 4.6 × 250 mm, Phenomenex); injection volume, 200 μL; flow rate, 1 mL/min; eluent A, 0.05% TFA in water; eluent B, 0.05% TFA in CH_3CN; gradient, from 0%B to 30%B in 60 min, and at 80%B for 20 min; detection at 214 nm. The main peaks were collected and characterized by electrospray ionization/time of flight mass spectrometry (ESI-TOF).

2.5. Surface functionalization

A specific functionalization of glass coverslips (area: 2.25 cm^2) was carried out following the procedure reported in Fig. 1. The side-chain deprotection was obtained treating each sample with a solution of 10 mL TFA with 0.23 mL MilliQ water, 0.1 mL TES, and 0.25 mL EDT for 1 h [9]. The samples underwent the following washings: once in TFA, twice in acetone, three times in MilliQ water and finally twice in acetone. The glass coverslips were dried under vacuum for 15 min.

2.6. Biological assays

2.6.1. Cell culture

Human (h) osteoblast cells were obtained from explants of cortical mandible bone collected during a surgical procedure from a healthy 38-year-old male subject. The study was approved by the Ethical Committee of the University Hospital of Padova. The patient was informed of the study aims and protocol and gave his written informed consent. Bone fragments were cultured in DMEM (Gibco) medium supplemented with heat inactivated FBS and incubated at 37 °C until cells migrated from the bone fragments. At cell confluence, bone fragments were removed, cells were detached using trypsin–EDTA (Gibco) and cultured in complete medium supplemented with 50 μg/mL ascorbic acid, 10 nM dexametasone, and 10 mM β-glycerophosphate (all purchased from Sigma-Aldrich). Osteoblast phenotype was confirmed by the von Kossa staining [37]. In this study h-osteoblasts were used at passage 5^{th}–8^{th} in culture. Cells (1.3 × 10^5 cells/cm^2) were seeded onto

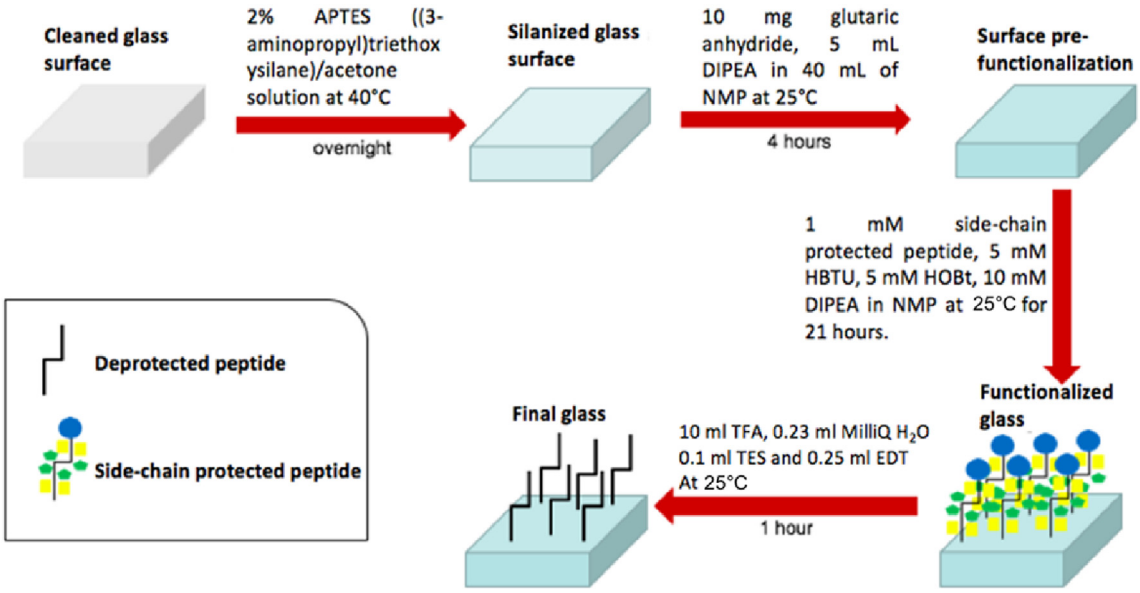

Fig. 1. Scheme of the covalent and specific functionalization of glass.

functionalized glass coverslips in complete culture medium. To avoid bacterial contamination, glass coverslips were previously incubated in ethanol 20% for 10 min and then extensively washed in sterile phosphate buffered saline (PBS). Cultures were then incubated for different time extent as specified for each experiment in a humidified tissue culture incubator (Heraeus; Corston, Bath, UK) at 37 °C in 5% CO_2 and 95% humidity. The incubator was also equipped with an additional pan of sterile water to prevent evaporation of tissue culture media. The volume and the pH of the complete medium were visually checked every 24 h.

2.6.2. Cell viability assay

Cellular viability was assessed using the MTT (3-(4,5-dimethylthia- zole-2-yl)-2,5-diphenyl tetrazoliumbromide; Sigma) assay on h-osteoblasts seeded on functionalized glass coverslips and incubated at 37 °C for 2 h, incubation time previously reported ensuring the optimal adhesion of h-osteoblasts to functionalized surfaces [9]. At the end of incubation, cells were rinsed three times with PBS in order to remove non-adherent cells and then incubated with MTT (5 mg/mL in 100 μL final volume) at 37 °C for 4 h. Reaction was stopped by adding 0.01 N HCl in 10% v/v SDS. To quantify adherent cells, a standard curve was obtained in each experiment by seeding a known number of h-osteoblasts. Absorbance of cells lysates were recorded at 620 nm.

2.6.3. Total internal reflection fluorescence (TIRF) microscope analysis

Human osteoblasts were cultured for 2 h at 37 °C on glass coverslips functionalized with adhesive peptides. The cells were then probed with FM 1–43 fluorescent dye (Invitrogen) able to insert into the outer leaflet of the cell membrane and then examined using an inverted microscope equipped with commercial white light TIRF apparatus (Nikon Instruments). The total internal reflection (TIR) at the glass coverslip–water interface was obtained using an objective based approach (CFI Plan Apochromat TIRF 60 × /1.45 oil) with a theoretical penetration depth from ~80–200 nm. Images were taken starting 1 min after the probe was added using a 2 megapixel CCD camera DS-2MBWc (Nikon Instruments, USA). To ensure optimal conditions, during acquisition cells were kept in a top-stage incubator (Tokai Hit, Japan) with temperature and CO_2 levels at 37 °C and 5%, respectively.

2.6.4. Immunocytochemistry

To deeply investigate cell adhesion and cell shape descriptors, human osteoblasts were cultured for 24 h or 96 h on functionalized glass coverslips. Cells were fixed in 4% w/v paraformaldehyde (PFA) for 10 min and then washed three times (5 min each) in PBS. Cells were permeabilized with 0.1% Triton X-100 and nonspecific binding sites were then blocked by incubation with 2% bovine serum albumin in TBS for 30 min. To label F-actin filaments cells were incubated with Phalloidin conjugated with tetramethyl rhodamine B isothiocyanate (TRITC; 50 μg/mL, Sigma-Aldrich). Following extensive washes, the samples were then washed, mounted, analysed, and photographed using a Leica TCSNT/SP2 confocal microscope. The images were digitally stored using Leica software.

For image analysis, single randomly chosen cells were contoured and shape parameters (area, perimeter, circularity, and convexity) were obtained using NIH Image J software [38].

2.6.5. Quantitative real time polymerase chain reaction

Specific mRNA transcript levels coding human Integrin Binding Sialoprotein (IBSP), human Vitronectin (VTN), and Secreted Phosphoprotein 1 (SPP1), were quantified in osteoblast cells cultured for 48 h on differently functionalized glass coverslips. At the end of incubation, total RNA was extracted using the SV Total RNA Isolation System kit (Promega, Milan, Italy). Contaminating DNA was removed by DNase I digestion. cDNA synthesis and subsequent polymerization was performed in a one-step using the iTaq Universal SYBR Green One-Step Kit (Bio-Rad). The reaction mixture contained 200 nM forward primer, 200 nM reverse primer, iTaq universal SyBR Green reaction mix, iScript reverse transcriptase, and 200 ng total RNA. Real time PCR was performed using ABI PRISM 7700 Sequence Detection System (Applied Biosystems). Data were quantified by the $\Delta\Delta^{CT}$ method using hGAPDH as reference gene. Target and reference genes were amplified with efficiencies near 100%. Oligonucleotides used for PCR are listed in Table 2.

2.6.6. Wester blotting

Human osteoblasts cultured for 24 h or 96 h on functionalized coverslips were washed twice in cold PBS and added of RIPA buffer

Table 2
Oligonucleotides used in this study. [a]Fw: forward; [b]Rv: reverse.

Gene [accession#]	Sequence
GAPDH	[a]Fw: 5′-cgggaagcccatcacca-3′
[NM_002046]	[b]Rv: 5′-ccggcctcaccccatt-3′
IBSP	Fw: 5′-ttactaccaccaccagtgaagc-3′
[NM_004967]	Rv: 5′-gatgcaaagccagaatggat-3′
VTN	Fw: 5′- ggaggacatcttcgagcttct-3′
[NM_000638]	Rv: 5′- gctaatgaactggggctgtc-3′
SPP1	Fw: 5′- aagtttcgcagacctgacatc-3′
[NM_000582]	Rv: 5′- ggctgtcccaatcagaagg-3′

(150 mM NaCl, 50 mM Tris-HCl, 0.25% w/v sodium deoxycholate, 0.1% Nonidet P-40, 100 μM NaVO4, 1 mM NaF, 1 mM phenylmethylsulfonyl fluoride, 10 μg/mL aprotinin, 10 μg/mL leupeptin). Cells were collected using cell scrapers and mechanically broken by vortexing and passing through pipette tips. Particulate material was removed by centrifugation and protein concentration was determined using bicinchoninic acid method (Pierce). Proteins (20μg/line) were separated in 10% SDS PAGE and then transferred to nitrocellulose membranes (Bio-Rad) in transfer buffer. Membranes were saturated in 5% milk in PBS containing 0.05% Tween-20 and probed with goat anti-focal adhesion kinase Ser 722 (p-FAK) antibody or with goat polyclonal anti-osteopontin (OPN, 1:500; Sigma-Aldrich) antibody to detect the protein encoded by the SPP1 gene. Following incubation at 4 °C for 16 h, membranes were extensively washed and incubate with the proper HRP-conjugated secondary antibodies. As loading control, membranes were stripped and re-probed with mouse monoclonal anti-beta actin antibody (1:5.000, Sigma-Aldrich). Bands were visualized using enhanced chemiluminescence (Millipore). Images were captured using Hyper Film MP (GE Healthcare) and densitometry analysis was performed using NIH Image J software.

2.6.7. Calcium assay

A hallmark of osteoblast differentiation and proliferation is the formation and deposition of calcium phosphate crystals [39]. As previously reported calcium content is undetectable at 2 days of culture, peaks at 7 days, and decreases at 14 days [40]. Therefore, in this study, calcium levels were assessed in h-osteoblasts cultured on differently functionalized glass coverslips for 7 days. During the incubation time, the complete medium was replaced every 48 h.

To assess calcium content, cultures were washed in PBS and incubated for 30 min at 4 °C with 5% (w/v) trichloroacetic acid (Sigma). Cell extracts (100 μL) were then combined with HCl 3.6 mM, *o*-cresolphthalein complexone 100 μM, 2-amino-2methyl-1-propanol 0.142 g/mL (all provided by Sigma). A standard curve was obtained by serial dilution (30-0 mg) of $CaCO_3$ solution. The absorbance was recorded at 620 nm. Calcium levels were normalized to protein concentration determined in the cell extracts using bicinchoninic acid method (Pierce, Thermo Fisher Scientific).

To further assess calcium deposition, cells were cultured as above described and fixed in 4% w/v PFA for 10 min at room temperature. Cells were washed with 1× PBS (pH 4.2) 3 times and then incubated with 2% w/v alizarin red S (sodium alizarin sulphonate) solution for 10 min at 37 °C. Alizarin red S was removed. Cells were rinsed with PBS 3 times and examined and photographed using a light microscope (Nikon, objective 10×) [41].

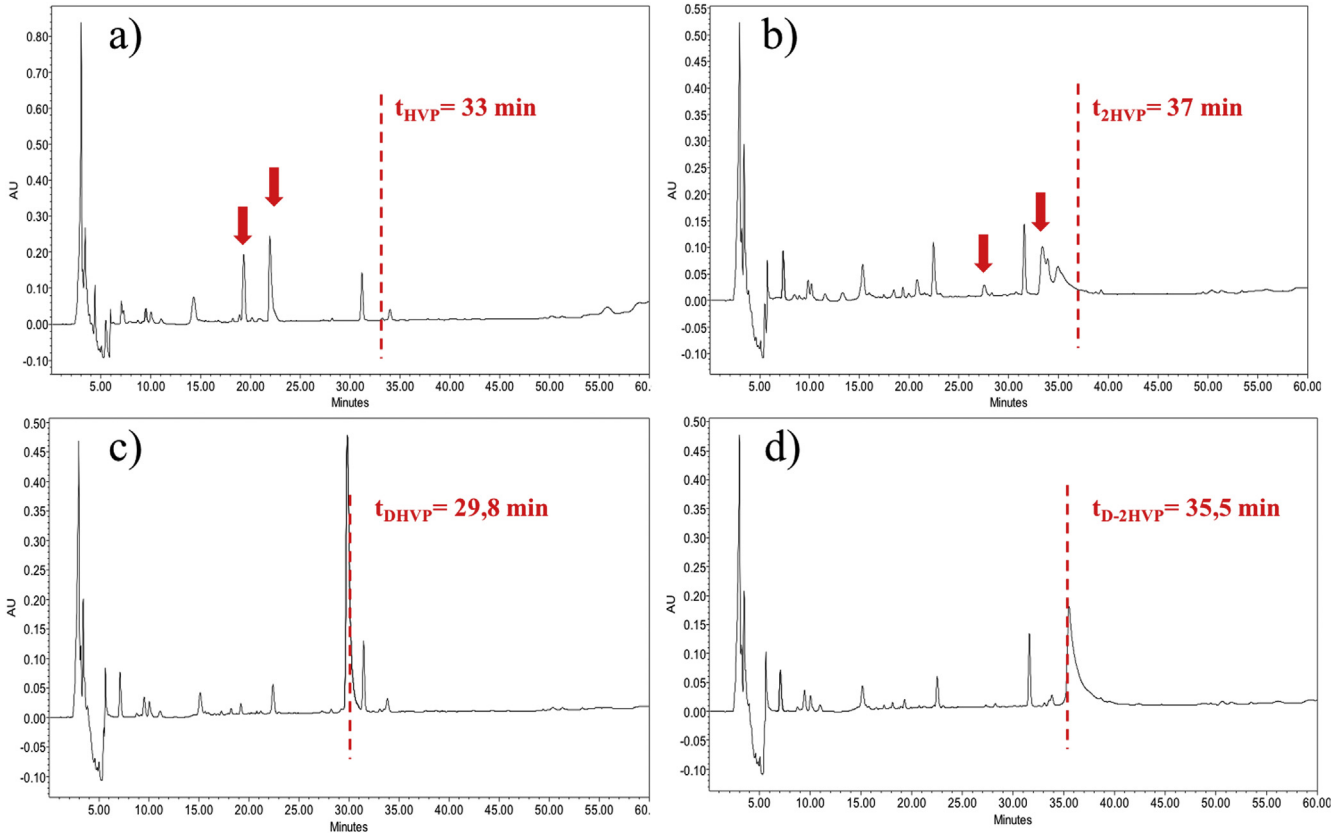

Fig. 2. Enzymatic degradation. Analytical HPLC chromatograms of HVP (a), 2HVP (b), DHVP (c) and D-2HVP (d), in 10% FBS at 37 °C after 5 h. Dotted lines indicate the retention time of each peptide in water at the same conditions of analysis. Other peaks in the chromatograms are due to serum components. Conditions: Column, Jupiter C_{18} "proteo" (4 μm, 90 Å, 4.6 × 250 mm); flow, 1 mL/min; eluent A, 0.05% TFA in H_2O milliQ; eluent B, 0.05% TFA in CH_3CN; injection, 200 μL; gradient, from 0 to 30% of B in 60 min; λ = 214 nm.

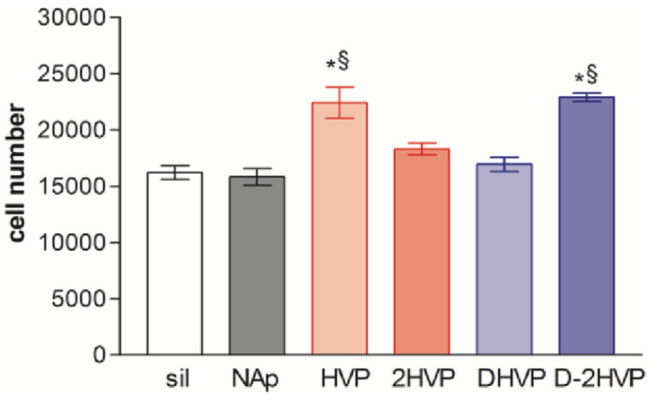

Fig. 3. h-Osteoblast adhesion. Evaluation of h-osteoblast adhesion on functionalized glass surfaces. Cells were seeded on functionalized glass surfaces and adhesion was evaluated by MTT test at 2 h. Cell number was calculated by plotting data to a standard curve. Data are expressed as the mean ± standard error of three independent experiments, each measured in duplicate. Sil: silanized surface. $^{*}P < 0.05$ *vs* osteoblasts seeded on glass-surface functionalized with a non-adhesive peptide NAp; $^{\S}P < 0.05$ *vs* osteoblasts seeded on silanized glass surface.

2.6.8. Statistical analysis

Biological data are reported as mean ± standard error. Statistical analysis was performed using the One-way ANOVA test followed by Bonferroni's multicomparison test, using Graph-Pad Prism 3.03. *P*-values <0.05 were considered statistically significant.

3. Results

3.1. Peptide density

The peptide density of HVP on glass surfaces was previously determined by a radiolabelling procedure and resulted 6.95 pmol cm^{-2} [9]. A comparable peptide density might derive from the application of the same procedure to the three proposed analogues.

3.2. Enzymatic degradation

The HVP treatment with 10% FBS for 5 h produces the complete fragmentation of the sequence. As shown in Fig. 2a, the peak of HVP, at retention time (t_R) = 33 min, completely disappears, whilst other less intense peaks appear at lower retention times. Peaks at t_R = 19.3 min and t_R = 21.9 min were identified as fragments GY (MW: 239 Da) and HRNRKGY (MW: 929 Da) respectively by ESI-TOF mass analysis. In a similar way (Fig. 2b), the L-dimer 2HVP was completely cleaved by serum enzymes, and the main fragments collected and identified were: KGYFRHRNR (t_R = 27.5 min, MW: 1232 Da, ESI-TOF) and FRHRNRKGYFRHRNR (t_R = 33.4 min, MW: 2099 Da, ESI-TOF). On the other side, both retro-inverted analogues were not degraded. HPLC chromatograms of retro-inverted peptides DHVP and D-2HVP after 5 h of treatment with 10% FBS are reported in Fig. 2c and d: the peptides retention times and the peaks areas are equal than those registered before serum treatment. The identity of uncleaved retro-inverted peptides was confirmed by ESI-TOF mass analysis. The peptide stabilization after 5 h-treatment is relevant considering the capacity of these peptides to enhance the early steps of surface-cell interaction.

3.3. Biological evaluation

3.3.1. Adhesion

The capacity of adhesive peptides to promote early cell adhesion was compared (Fig. 3). Following 2 h culture, the native sequence (HVP) grafted to glass-surface significantly enhanced osteoblast adhesion as compared to surfaces functionalized with a non-adhesive peptide (NAp) and the silanized glass, as expected. Interesting, the adhesion of h-osteoblasts on the samples functionalized with the retro-inverted dimer D-2HVP was comparable to HVP one and significantly increased as compared to the controls ($P < 0.05$). On the contrary, the dimeric form of HVP (2HVP) and the retro-inverso peptide DHVP did not increased cell adhesion and data were comparable to the controls. In conclusion, the retro-inverted dimeric analogue reported adhesive performance comparable to those of native HVP peptide, whereas the L-dimeric form and the retro-inverted sequence of HVP did not improved cell adhesion in comparison with the control surfaces.

3.3.2. TIRF analysis

Attachment of human osteoblasts to functionalized glass surfaces was investigated by TIRF microscopy 2 h after cell seeding. As reported in Fig. 4, osteoblasts stained with FM 1–43 and seeded on silanized glass or DHVP functionalized surfaces reported weak fluorescent signals with few areas of increased dye concentration, indicating a homogenous adhesion pattern. Osteoblasts seeded on the dimeric analogues 2HVP and D-2HVP showed a unique distribution of fluorescent signals with an increased fluorescent intensity and signalling pattern localized to discrete areas of cell membrane consistent with focal adhesion formation. In addition,

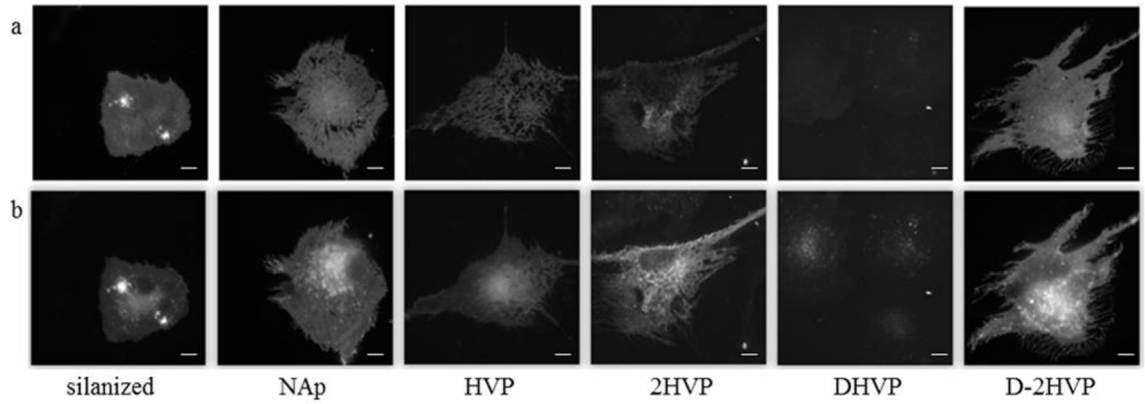

Fig. 4. TIRF microscopy. a) Epifluorescence on h-osteoblasts cultured for 2 h on functionalized glass coverslips. b) Cells were probed with FM 1–43 fluorescent dye. Images were taken using a 2 megapixel CCD with CFI Plan Apochromat TIRF 60×/1.45 oil objective. Representative photomicrographs, n = 3 per group. Scale bar 10 μm.

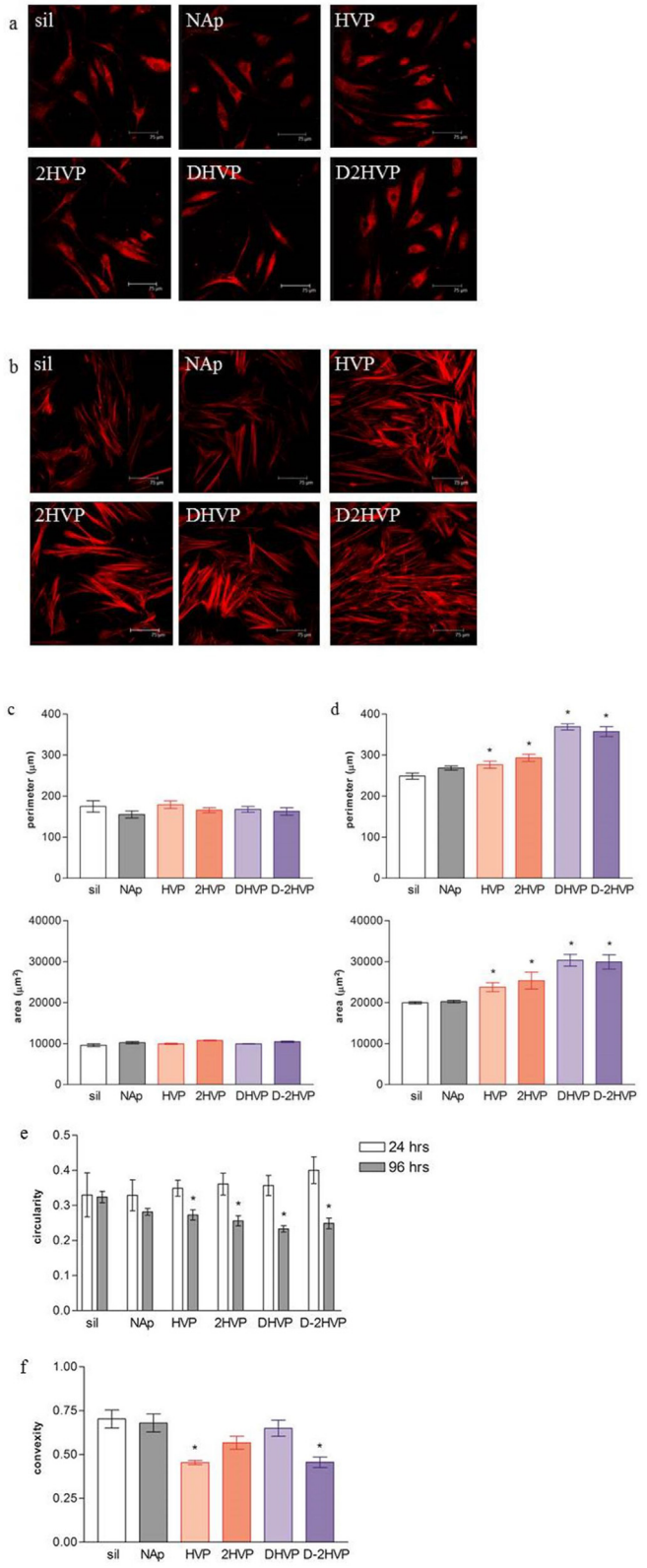

Fig. 5. Cell morphology. a) Confocal microscopy in h-osteoblasts cultured for 24 h (a) or 96 h (b) and stained with Phalloidin-TRITC. Representative images, n = 4 per group. Scale bar: 75 μm. Image analysis was performed on 4 images for each experimental group. Perimeter and area were obtained using NIH Image J software in cells cultured for 24 h (c) or 96 h (d). $^*P < 0.05$ *vs* osteoblasts seeded on silanized glass surfaces. e) Circularity was calculated as the ratio between the area and the square of the perimeter. $^*P < 0.05$ *vs* osteoblasts cultured for 24 h on respective functionalized glass surfaces. f) Convexity was calculated as the perimeter ratio of cells cultured for 24 h and 96 h $^*P < 0.05$ *vs* osteoblasts seeded on silanized glass surfaces. Sil: silanized surface.

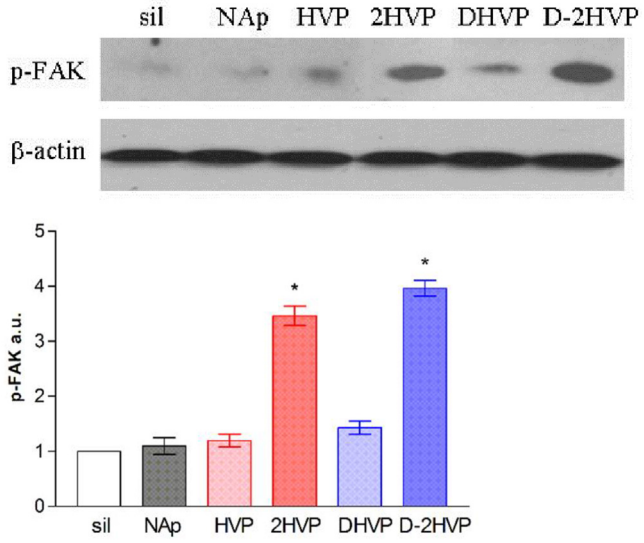

Fig. 6. FAK Ser722 phosphorylation. a) Western blot analysis on h-osteoblasts cultured for 24 h to evaluate Ser722 phosphorylation of focal adhesion kinase (p-FAK) and expression of β-actin as loading control. Representative images of 3 experiments. b) Proteins signals were determined by densitometry. β-actin was used to normalized signals. $^*P < 0.05$ vs osteoblasts seeded on silanized glass surfaces. Sil: silanized surface.

the dimeric analogues grafted to glass surfaces fostered a dense formation of membrane structures protruding from the osteoblast cells resembling filopodia, slender membrane projections extending beyond the leading edge in migrating cells [42].

3.3.3. Cellular morphology

Human osteoblasts cultured for 24 h on functionalized coverslips revealed comparable arrangement of cytoskeletal components as demonstrated by fluorescent signals relative to Phalloidin (Fig. 5, a). On the contrary, following 96 h in culture the F-actin fibers were organized in straight structures which overlapped in cells cultured on HVP, DHVP, and D-2HVP functionalized surfaces (Fig. 5, b). At the same, perimeter and area did not differ in cells cultured on different functionalized coverslips for 24 h. However, human osteoblasts cultured for 96 h on HVP, 2HVP, DHVP, and D-2HVP showed significantly higher perimeter and area values as compared with cells seeded on silanized or NAp functionalized surfaces (Fig. 5c and d). Comparing cells cultured for 24 h or 96 h, circularity values decreased over the time only in cells seeded on HVP, 2HVP, DHVP, and D-2HVP (Fig. 5, e). Basically, the lower circularity values are, the higher the trend for cells to protrude and migrate, thus making cell boundaries more complex. Convexity, calculated as the perimeter ratio at 24 h and 96 h, indicates the relative deviation of cell shape from a convex object. In our experiments, cells cultured on HVP and D-2HVP showed decreased convexity (Fig. 5, f), thus suggesting an enlargement of cell surface area in comparison to the occupied space.

3.3.4. Focal adhesion

To further investigate the interaction of human osteoblasts with functionalized glass surfaces, FAK Ser722 phosphorylation was assessed by Western blot analysis on cells cultured for 24 h. As reported in Fig. 6, p-FAK increased in osteoblasts cultured on HVP and D-2HVP as compared with cells seeded on the other

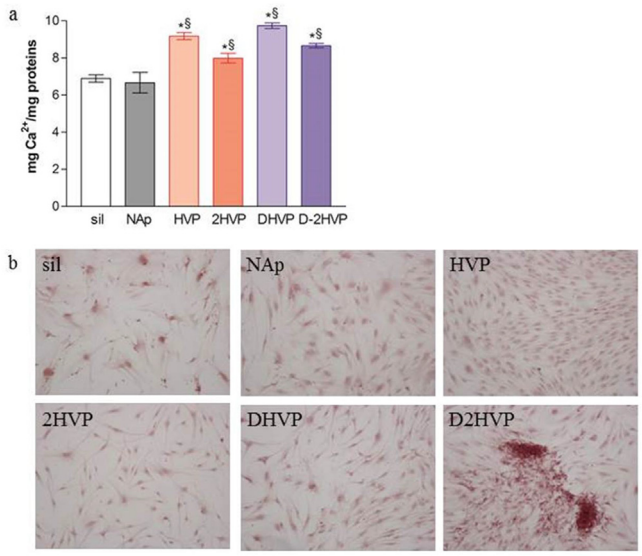

Fig. 7. Calcium levels. Calcium levels evaluated in h-osteoblasts cultured for 7 days onto differently functionalized glass coverslips. a) Calcium deposition was assessed by *o*-cresolphthalein complexone. Data are expressed as the mean ± standard error of three independent experiments, each measured in duplicate. *$P < 0.05$ *vs* osteoblasts seeded on glass-surface functionalized with a non-adhesive peptide NAp; §$P < 0.05$ *vs* osteoblasts seeded on silanized glass surface. b) Calcium deposition was visualized by alizarin red S staining. Images were acquired using a light microscope (Nikon, objective 10×). Representative images of 3 experiments. Sil: silanized surface.

functionalized surfaces. Densitometry analysis revealed a slight, non-statistically significant difference between the two cell cultures.

3.3.5. Mineralization and osteogenic differentiation

During the osseointegration process, cell adhesion is the early step whereas cell differentiation and mineralization of extracellular matrix eventually determine the success of the implant [36]. Since levels of calcium deposited by cells are indicative of cell differentiation and mineralization of bone matrix, in this study calcium was assessed on h-osteoblasts cultured for 7 days on different functionalized surfaces. As reported in Fig. 7 panel a, all functionalized surfaces increased calcium deposits compared to cells cultured on silanized glass or glass functionalized with non-adhesive peptide. H-osteoblasts cultured on surfaces grafted with HVP and DHVP reported a more evident calcium deposition. Mineralization of extracellular matrix was assessed also by alizarin red S staining. As reported in Fig. 7 panel b, calcium deposits were clearly evident in osteoblasts cultured for 7 days on D-2HVP functionalized glass surfaces.

To further evaluate the role of different functionalized surfaces in sustaining h-osteoblast differentiation, expression of genes involved in bone formation was evaluated by quantitative RT-PCR. As reported in Fig. 8, HVP, 2HVP and D-2HVP increased mRNA specific transcript levels coding integrin binding sialoprotein (IBSP), a major structural protein of the bone matrix involved in cell attachment [43]. Interestingly, mRNA transcript levels coding secreted phosphoprotein 1 (SPP1) or osteopontin, involved in bone mineralization and remodelling, increased in h-osteoblasts cultured on HVP or D-2HVP functionalized surfaces whereas vitronectin (VTN) mRNA levels augmented only in cells cultured on D-2HVP. IBSP, VTN and SPP1 gene expressions did not increase in cells cultured on NAp samples as compared to silanized glass.

The increased in mRNA transcript levels specific for SPP1 was confirmed by Western blot analysis on human osteoblasts cultured for 96 h. As reported in Fig. 9, expression of osteopontin increased

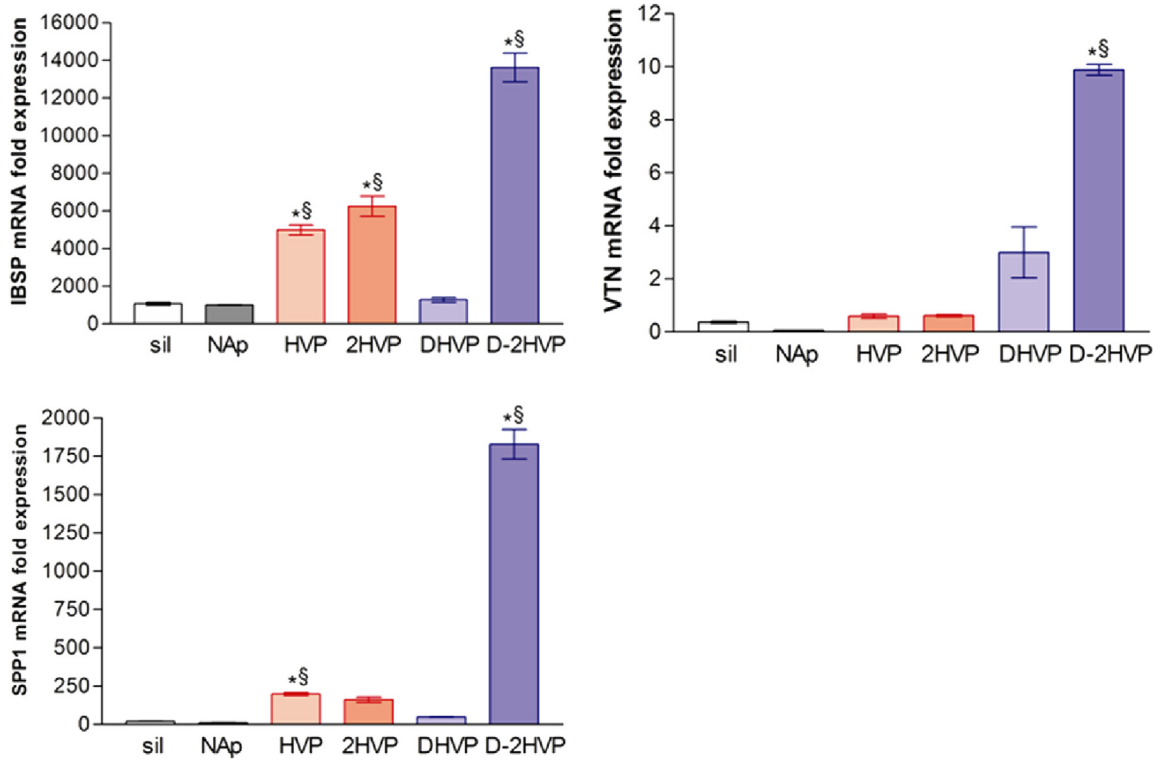

Fig. 8. Gene expression. a) Human *IBSP* (Integrin-Binding Sialoprotein), b) human *VTN* (Vitronectin) and c) *SPP1* (secreted phosphoprotein-1) mRNA specific transcript levels evaluated by quantitative RT-PCR. Data are expressed as the mean ± standard error of two independent experiments, each measured in duplicate. Sil: silanized surface. *$P < 0.05$ *vs* osteoblasts seeded on glass-surface functionalized with a non-adhesive peptide NAp; §$P < 0.05$ *vs* osteoblasts seeded on silanized glass surface.

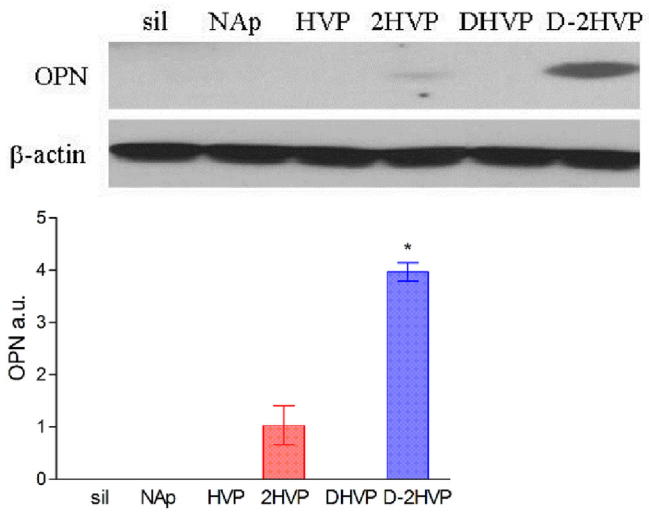

Fig. 9. Osteopontin protein expression. a) Western blot analysis on h-osteoblasts cultured for 96 h to evaluate expression of osteopontin (OPN) and β-actin as loading control. Representative images of 3 experiments. b) Proteins signals were determined by densitometry. β-actin was used to normalized signals. $^{*}P < 0.05$ *vs* osteoblasts seeded on silanized glass surfaces. Sil: silanized surface.

in cells cultured on D-2HVP. Densitometry analysis revealed that increased in protein expression was statistically different in cells cultured on D-2HVP but not in cells cultured on HVP as compared to cells cultured on silanized glass.

4. Discussion

During osteoconduction and osseointegration the interaction of cells with the surface of the implant is mainly regulated by the accessibility and stability of adhesion sites. The images obtained by TIRF microscopy (Fig. 4) indicated that, unlike DHVP, surfaces functionalized with HVP, 2HVP and D-2HVP affect cell shape imprinting a non-rounding jagged profile enriched in membrane protrusions (Fig. 5). Indeed, organization of cytoskeleton and formation of filopodia are indicative of migrating cells which are sensing the extracellular environment looking for cues of spreading and colonization. However, cells attach to HVP and D-2HVP form focal contacts (Figs. 4 and 6) suggesting that different conformations/accessibility/flexibility of peptides interact with specific cellular membrane structures to guide unique biological responses. Except for the adhesion assay, the peptide 2HVP behaves exactly the same as its monomer: the duplication of the sequence does not seem to increase the ionic interactions between the peptide and osteoblast surface glycosaminoglycans. Nevertheless, by TIRF analysis cells on 2HVP attach (Fig. 4) more closely than HVP: on 2HVP-surface few cells adhere but they are well anchored. On the other hand, the retro-inverted peptide DHVP shows a different bioactivity compared to L-peptide: a reduced ability to mediate adhesion, similar mineralization, the inability to increase the gene expression of IBSP and SPP1. The absence of the enzymatic degradation for DHVP-surface is combined with a different biological activity compared to that of HVP-surface. This is also confirmed by the cell morphological analysis: HVP induces the formation of filopodia in adherent cells, while the cells on glass functionalized with DHVP appear difficult to distinguish and much more rounded-shape. The failure in ensuring the analogous retro-inverso the same biological properties of the L-peptides is described in the literature for sequences that assume α-helical conformations but this is not the case, as HVP assumes a β-turn structure involving the sequence (5–8) [44]. A conformational analysis (CD, NMR and Raman) of the different peptides both in solution and grafted to glasses, is in progress for determining the role of the secondary structure of each analogue in its biological activity. Surprisingly similar biological properties of the HVP-surface are found in the D-2HVP-surface. In particular, an equal adhesive strength joins an increased gene expression of all three genes tested. The TIRF images showed a strong adhesion of osteoblasts on D-2HVP surfaces and proved the existence of many focal contacts. The possibility that the 9-mer sequence of the dimeric molecule closer to the surface could constitute a kind of spacer able to improve the interaction between the peptide and the cellular GAGs is currently under study even if the synergistic effect of multi-copy conjugate of retro-inverso peptides was demonstrated [45]. The bioactivity of HVP peptide has previously proved to be particularly significant in the early stages of the interaction between the cells and the functionalized surfaces [9,19]: the adhesive property, restricted to short times, might be influenced to the degradation of the sequence. Further studies of surfaces functionalized with the retro-inverted D-2HVP will clarify whether, in the absence of enzymatic cleavage, the benefits due to the adhesive peptide presence will be extended in time and will change the successive phases of the cell population such as migration, differentiation and growth.

5. Conclusions

In this study, three analogues of h-Vitronectin nonapeptide HVP were designed and synthetized for glass surface covalent and selective functionalization. The goals were (i) to improve the bioactivity by increasing the ionic interaction between peptide and cellular GAGs, and (ii) to increase the life-time of these sequences under physiological conditions. To achieve the first goal (i), a dimeric analogue of HVP sequence was synthetized (2HVP); in order to obtain the second purpose (ii) two retro-inverted sequences, one as monomer and the other as dimer (DHVP and D-2HVP), were prepared. We demonstrated that sequence duplication did not improve HVP bioactivity. Unlike L-peptides, retro-inverted peptides were not degraded by fetal bovine serum proteolytic enzymes. More important, D-2HVP, grafted to glass surfaces, efficiently improves h-osteoblasts adhesion and spread, increases intracellular calcium levels and stimulates expression of integrin binding sialoprotein, vitronectin and secreted phosphoprotein 1, proteins involved in bone formation. Finally, osteoblasts cultured on D-2HVP-functionalized glasses showed focal adhesion contacts with the surfaces and elongated cellular shape with several protrusions confirming the role of this retro-inverted peptide in presenting proper extracellular cues.

Acknowledgements

The authors would like to thank Dr. Margherita Giovine for her help in the peptide synthesis and surface functionalization, and Dr. Alessio Broccanello for the enzymatic degradation tests. We thank Yoav Luxembourg (Luxembourg Bio Technologies Ltd) for the generous gift of coupling reagents.

References

[1] T. Meling, K. Harboe, K. Søreide, Incidence of traumatic long-bone fractures requiring in-hospital management: a prospective age- and gender-specific analysis of 4890 fractures, Injury 40 (2009) 1212–1219.
[2] M. Hallman, A. Thor, Bone substitutes and growth factors as an alternative/complement to autogenous bone for grafting in implant dentistry, Periodontol 2000 47 (2008) 172–192.
[3] D. Rickert, J.J. Slater, H.J. Meijer, A. Vissink, G.M. Raghoebar, Maxillary sinus lift with solely autogenous bone compared to a combination of autogenous bone and growth factors or (solely) bone substitutes. A systematic review, Int. J.

Oral Maxillofac. Surg. 41 (2012) 160–167.
[4] E. Nkenke, V. Weisbach, E. Winckler, P. Kessler, S. Schultze-Mos-gau, J. Wiltfang, F.W. Neukam, Morbidity of harvesting of bone grafts from the iliac crest for preprosthetic augmentation procedures: a prospective study, Int. J. Oral Maxillofac. Surg. 33 (2004) 157–163.
[5] A. Barone, M. Ricci, F. Mangano, U. Covani, Morbidity associated with iliac crest harvesting in the treatment of maxillary and mandibular atrophies: a 10-year analysis, J. Oral Maxillofac. Surg. 69 (2011) 2298–2304.
[6] B. Al-Nawas, E. Schiegnitz, Augmentation procedures using bone substitute materials or autogenous bone - a systematic review and meta-analysis, Eur. J. Oral Implantol. 7 (Supplement 2) (2014) 219–234.
[7] A.R. Amini, C.T. Laurencin, S.P. Nukavarapu, Bone tissue engineering: recent advances and challenges, Crit. Rev. Eng. 40 (2012) 363–408.
[8] D.E. Hughes, D.M. Salter, S. Dedhar, R. Simpson, Integrin expression in human bone, J. Bone Min. Res. 8 (1993) 527–533.
[9] P. Brun, M. Scorzeto, S. Vassanelli, I. Castagliuolo, G. Palù, F. Ghezzo, G.M.L. Messina, G. Iucci, V. Battaglia, S. Sivolella, A. Bagno, G. Polzonetti, G. Marletta, M. Dettin, Mechanisms underlying the attachment and spreading of human osteoblasts: from transient interactions to focal adhesions of vitronectin-grafted bioactive surfaces, Acta Biomater. 9 (2013) 6105–6115.
[10] M. Ramazanoglu, Y. Oshida, Osseointegration and Bioscience of Implant Surfaces - Current Concepts at bone-Implant Interface in “Implant Dentistry - a Rapidly Evolving Practice, 2011, pp. 57–83 chapter 3, Published by InTech.
[11] R. Hassert, A.G. Beck-Sickinger, Tuning peptide affinity for biofunctionalized surfaces, Eur. J. Pharm. Biopharm. 85 (2013) 69–77.
[12] S. Bierbaum, V. Hintze, D. Scharnweber, Functionalization of biomaterial surfaces using artificial extracellular matrices, Biomatter 2 (2012) 132–141.
[13] R. Beutner, J. Michael, B. Schwenzer, D. Scharnweber, Biological nanofunctionalization of titanium based biomaterial surfaces: a flexible toolbox, J. R. Soc. Interface 7 (2010) 93–105.
[14] M. Dettin, A. Zamuner, G. Iucci, G.M.L. Messina, C. Batocchio, G. Picariello, G. Gallina, G. Marletta, I. Castagliuolo, P. Brun, Driving h-osteoblast adhesion and proliferation on titania: peptide hydrogels decorated with growth factors and adhesive conjugates, J. Pept. Sci. 20 (2014) 585–594.
[15] K.E. Sapsford, W.R. Algar, L. Berti, K.B. Gemmill, B.J. Casey, E. Oh, M.H. Stewart, I.L. Medintz, Functionalizing nanoparticles with biological molecules: developing chemistries that facilitate nanotechnology, Chem. Rev. 113 (2013) 1904–2074.
[16] M. Dettin, T. Herath, R. Gambaretto, G. Iucci, C. Batocchio, A. Bagno, F. Ghezzo, C. Di Bello, G. Polzonetti, L. Di Silvio, Assessment of novel chemical strategies for covalent attachment of adhesive peptides to rough titanium surfaces: XPS analysis and biological evaluation, J. Biomed. Mater. Res. A 91 (2009) 463–479.
[17] A. Bagno, A. Piovan, M. Dettin, A. Chiarion, P. Brun, R. Gambaretto, G. Fontana, C. Di Bello, G. Palù, I. Castagliuolo, Human osteoblast-like cells adhesion on titanium substrates covalently functionalized with synthetic peptides, Bone 40 (2007) 693–699.
[18] G. Maheshwari, G. Brown, D.A. Lauffenburger, A. Wells, L.G. Griffith, Cell adhesion and motility depend on nanoscale RGD clustering, J. Cell. Sci. 113 (2000) 1677–1686.
[19] A. Cacchioli, F. Ravanetti, A. Bagno, M. Dettin, C. Gabbi, Human vitronectin-derived peptide covalently grafted onto titanium surface improves osteogenic activity: a pilot in vivo study on rabbits, Tissue Eng. Part A 15 (2009) 2917–2926.
[20] J. Conde, J.T. Dias, V. Grazú, M. Moros, P.V. Baptista, J.M. de la Fuente, Revisiting 30 years of biofunctionalization and surface chemistry of inorganic nanoparticles for nanomedicine, Front. Chem. 15 (2014) 2–48.
[21] M. Tallawi, E. Rosellini, N. Barbani, M.G. Cascone, R. Rai, G. Saint-Pierre, A.R. Boccaccini, Strategies for the chemical and biological functionalization of scaffolds for cardiac tissue engineering: a review, J. R. Soc. Interface 12 (108) (2015) 20150254, 6.
[22] M. Dettin, A. Bagno, R. Gambaretto, G. Iucci, M.T. Conconi, N. Tucitto, A.M. Menti, C. Grandi, C. Di Bello, A. Licciardello, G. Polzonetti, Covalent surface modification of titanium oxide with different adhesive peptides: surface characterization and osteoblast-like cell adhesion, J. Biomed. Mater. Res. 90 (2009) 35–45.
[23] E. Battista, F. Causa, V. Lettera, V. Panzetta, D. Guarnieri, S. Fusco, F. Gentile, P.A. Netti, Ligand engagement on material surfaces is discriminated by cell mechanosensoring, Biomaterials 45 (2015) 72–80.
[24] S. Esposito, R. Mele, R. Ingenito, E. Bianchi, F. Bonelli, E. Monteagudo, L. Orsatti, An efficient liquid chromatography-high resolution mass spectrometry approach for the optimization of the metabolic stability of therapeutic peptides, Anal. Bioanal. Chem. (2017), http://dx.doi.org/10.1007/s00216-017-0213-1.
[25] P. Zubrzak, H. Williams, G.M. Coast, R.E. Isaac, G. Reyes-Rangel, E. Juaristi, J. Zabrocki, J. Nachman, β-amino acid of an insect neuropeptide feature potent bioactivity and resistance to peptidase hydrolysis, Biopolymers 88 (2007) 76–82.
[26] Y. Li, Y. Lei, E. Wagner, C. Xie, W. Lu, J. Zhu, J. Shen, J. Wang, M. Liu, Potent retro-inverso D-peptide for simultaneous targeting of angiogenic blood vasculature and tumor cells, Bioconjugate Chem. 24 (2013) 133–143.
[27] V. Parhsarathy, P.L. McClean, C. Holscher, M. Taylor, C. Tinker, G. Jones, O. Kolosov, E. Salvati, M. Gregori, M. Masserini, D. Allsop, A novel retro-inverso peptide inhibitor reduces amyloid deposition, oxidation and inflammation and stimulates neurogenesis in the APPswe/PS1ΔE9 mouse model of Alzheimer's disease, Plos One 8 (2013) e54769.
[28] K.R. Ngoei, B. Catimel, N. Milech, P.M. Watt, M.A. Bogoyevitch, A novel retro-inverso peptide is a preferential JNK substrate-competitive inhibitor, Biochem. Cell Biol. 45 (2013) 1939–1950.
[29] A.K. Carmona, L. Juliano, Inhibition of angiotesin converting enzyme and potentiation of bradykinin by retro-inverso analogues of short peptides and sequences related to angiotesin I and bradykinin, Biochem. Pharmacol. 51 (1996) 1051–1060.
[30] C. de la Fuente-Núñez, F. Reffuveille, S.C. Mansour, S.L. Reckseidler-Zenteno, D. Hernández, G. Brackman, T. Coenye, R.E. Hancock, D-enantiomeric peptides that eradicate wild-type and multidrug-resistant biofilms and protect against lethal Pseudomonas aeruginosa infections, Chem. Biol. 19 (2) (2015) 196–205, 22.
[31] C. Li, M. Pazgier, J. Li, C. Li, M. Liu, G. Zou, Z. Li, J. Chen, S.G. Tarasov, W.Y. Lu, W. Lu, Limitations of peptide retro-inverso isomerization in molecular mimicry, J. Biol. Chem. 18 (25) (2010) 1957281, 285.
[32] D.T. Nair, K.J. Kaur, K. Singh, P. Mukherjee, D. Rajagopal, A. George, V. Bal, S. Rath, K.V. Rao, D.M. Salunke, Mimicry of native peptide antigens by the corresponding retro-inverso analogs is dependent on their intrinsic structure and interaction propensities, J. Immunol. 170 (2003) 1362–1373.
[33] J. Wang, Y. Lei, C. Xie, W. Lu, E. Wagner, Z. Xie, J. Gao, X. Zhang, Z. Yan, M. Liu, Retro-inverso CendR peptide-mediated polyethyleneimine for intracranial glioblastoma-targeting gene therapy, Bioconjugate Chem. 25 (2014) 414–423.
[34] J. Gu, X. Chen, X. Fang, X. Sha, Retro-inverso D-peptide-modified HA/RHB/pDNA core-shell ternary nanoparticles for the dual-targeted delivery of short hairpin RNA-encoding plasmids, Acta Biomater. (2017), http://dx.doi.org/10.1016/j.actbio.2017.04.024.
[35] M. Dettin, M.T. Conconi, R. Gambaretto, A. Bagno, C. Di Bello, A.M. Menti, C. Grandi, P.P. Parnigotto, Effect of synthetic peptides on osteoblast adhesion, Biomaterials 26 (2005) 4507–4515.
[36] M. Dettin, A. Bagno, R. Gambaretto, C. Di Bello, M.T. Conconi, P.P. Parnigotto, Peptidi della vitronectina e loro impiego terapeutico nella adesione degli osteoblasti, Italian patent n° PD 2004 A 000065, 2004.
[37] L.G. Luna, Manual of Histologic Staining Methods of the Armed Forces Institute of Pathology, McGraw-Hill, New York, Blakiston Division, 1968.
[38] J. Lobo, E.Y. See, M. Biggs, A. Pandit, An insight into morphometric descriptors of cell shape that pertain to regenerative medicine, J. Tissue Eng. Regen. Med. 10 (2016) 539–553.
[39] J. Ortiz, L.L. Chou, Calcium upregulated survivin expression and associated osteogenesis of normal human osteoblasts, J. Biomed. Mater. Res. A 100 (2012) 1770–1776.
[40] P. Brun, F. Ghezzo, M. Roso, R. Danesin, G. Palù, A. Bagno, M. Modesti, I. Castagliuolo, M. Dettin, Electrospun scaffolds of self-assembling peptides with poly(ethylene oxide) for bone tissue engineering, Acta Biomater. 7 (2011) 2526–2532.
[41] Y.H. Wang, Y. Liu, P. Maye, D.W. Rowe, Examination of mineralized nodule formation in living osteoblastic cultures using fluorescent dyes, Biotechnol. Prog. 22 (2006) 1697–1701.
[42] C.D. Nobes, A. Hall, Rho GTPases control polarity, protrusion, and adhesion during cell movement, J. Cell Biol. 144 (1999) 1235–1244.
[43] L.W. Fisher, O.W. McBride, J.D. Termine, M.F. Young, Human bone sialoprotein. Deduced protein sequence and chromosomal localization, J. Biol. Chem. 265 (1990) 2347–2351.
[44] G. Vacatello, L. D'Auria, M. Falcigno, R. Dettin, Gambaretto, C. Di Bello, L. Paolillo, Conformational analysis of heparin binding peptides, Biomaterials 26 (2005) 3207–3214.
[45] G. Zhang, M.J. Leibowitz, P.J. Sinko, S. Stein, Multiple-Peptide Conjugates for binding β-amyloid plaques of alzheimer's disease, Bioconjugate Chem. 14 (2003) 86–92.